CARBON 94 (2015) 485–493

Contents lists available at ScienceDirect

CARBON

journal homepage: www.elsevier.com/locate/carbon

Fabrication of DLC thin films with improved diamond-like carbon character by the application of external magnetic field

Ali Modabberasl [a], Parviz Kameli [a,*], Mehdi Ranjbar [a], Hadi Salamati [a], Rouholah Ashiri [b]

[a] Department of Physics, Isfahan University of Technology, Isfahan 84156-83111, Iran
[b] Department of Materials Engineering, Isfahan University of Technology, Isfahan 84156-83111, Iran

ARTICLE INFO

Article history:
Received 15 February 2015
Received in revised form 20 May 2015
Accepted 30 June 2015
Available online 2 July 2015

Keywords:
Diamond-like carbon
Pulsed laser deposition
Magnetic field
Ionization

ABSTRACT

Diamond-like carbon (DLC) thin films were grown on Si-(100) substrates by a magnetically-assisted pulsed laser deposition (PLD) technique. The role of magnetic field on the structural, morphological, mechanical properties and deposition rate of DLC thin films has been studied. The obtained films were characterized by Raman spectroscopy, X-ray photoelectron spectroscopy (XPS), atomic force microscopy (AFM), field emission scanning electron microscopy (FE-SEM) and nanoindentation techniques. It was found that the diamond-like character, thickness and deposition rate of the DLC films increase in the presence of magnetic field. The films deposited under magnetic field exhibit a denser microstructure and smoother surface with lower surface roughness. Meanwhile, the mechanical properties of the magnetically processed DLC thin films experience an improvement, relative to the conventionally processed ones. It seems that the DLC films deposited under magnetic field can be better candidate for hard and wear resistance coating applications.

© 2015 Elsevier Ltd. All rights reserved.

1. Introduction

Diamond-like carbon (DLC) thin films have attracted much interest due to their unique properties such as high hardness, low friction, good wear resistance, optical transparency and high chemical inertness [1–4]. Due to these excellent properties, DLC films have been widely used for several critical applications such as protective coatings for magnetic recording disks, cutting tools, optical components and micro-electromechanical devices (MEMs) [5–9]. The properties and the quality of the DLC thin films are strongly related to their microstructure, i.e., sp^3 and sp^2 bonding ratio in the carbon network [10–12]. In deposition process, energetic ion bombardment promotes sp^3 bonding. According to the sub-plantation model [1,13,14], low energy carbon ions cannot penetrate the surface and just stick to the surface resulting in the formation of amorphous sp^2-bonded carbon network [13]. During the deposition process, the incident carbon ion having a sufficient energy (beyond the penetration threshold) can only penetrate into the growing film. This carbon ion enters subsurface interstitial site and therefore, results in the increase of the local film density [1] and the development of compressive stress [15]. The local bonding will then reform around that atom according to this new density. In the highly energetic conditions of ion bombardment existing during film growth, atomic hybridizations will adjust easily according to the changes in the local density, and become more sp^2 if the density is low and more sp^3 if the density is high [1]. Thus, the energy and amount of ion species are the most effective factors determining the film growth and ratio of sp^3/sp^2 carbon atoms of the DLC films [1,16,17]. Significant attempts have been dedicated to improve the quality of DLC thin films by varying the deposition technique and also the process parameters [18,19]. In order to deposit a high quality, dense, and hard DLC thin film with a higher degree of the diamond-like character highly ionized plasma is needed.

Filtered cathodic vacuum arc (FCVA) [20–22] and pulsed laser deposition (PLD) [11,23,24], as energetic and plasma based deposition methods, have been used for the preparation of DLC films. For the formation of DLC film, FCVA process has some advantages such as generation of high energetic carbon species with a fairly narrow ion energy distribution, ability of low deposition temperature, and an industrial scale production capability [20,22]. However, in FCVA process, filtering is not sufficient for some applications and the cathode spot is unstable [1]. Pulsed laser deposition (PLD) is also an attractive technique for DLC films preparation because of its outstanding advantages such as simplicity of preparing a target, ability of low deposition temperature, low damage to the substrate, and ablation of energetic carbon species from graphite

* Corresponding author.
E-mail address: kameli@cc.iut.ac.ir (P. Kameli).

http://dx.doi.org/10.1016/j.carbon.2015.06.081
0008-6223/© 2015 Elsevier Ltd. All rights reserved.

target [11,23,24]. In the PLD process, the ablation plume contains many particles such as electrons, ions and neutral atoms. In order to achieve a high plasma density and an enhanced ionization of the ablated species during the expansion of laser-produced plasma, a magnetic field can be incorporated into conventional PLD technique. Kobayashi et al. developed a magnetically-assisted PLD technique (known as aurora method) to deposit $SrTiO_3$, NiO and ZnO thin films on different substrates [25–28]. They have showed that the aurora method increases the ionization of the growth species in the plume in the vicinity of the substrate. As far as we know, magnetically-assisted PLD technique has not been used for preparation of DLC thin films till now and is the main course of this work. It is expected that the magnetically-assisted PLD will improve the quality and properties of DLC films by the production of the highly ionized plasma during deposition process. We have tried to develop this method for obtaining high quality DLC films with enhanced diamond like character.

In this work, we have deposited DLC thin films by PLD technique in the presence of an external magnetic field normal to the substrate. Moreover, the effects of applied magnetic field on the structure, morphology and mechanical properties and deposition rate of the DLC thin films were studied. Raman spectroscopy and X-ray photoelectron spectroscopy (XPS) have been used to investigate the structural properties and chemical bonding state of the obtained DLC films. The mechanical properties, morphological features and deposition rate of the DLC films are studied using nanoindentation, atomic force microscopy (AFM) and field emission scanning electron microscopy (FE-SEM).

2. Experimental details

DLC thin films were deposited on ultrasonically cleaned single crystal Si-(100) substrates by PLD technique with and without the presence of non-homogeneous magnetic field. A commercially available pyrolytic graphite target with high purity was used as a target in the present work. The deposition chamber was evacuated to a base pressure of 1×10^{-6} Torr. A KrF excimer laser (wavelength 248 nm, 20 ns FWHM, 10 Hz repetition rate) with 200 mJ energy per pulse was used for the ablation of the rotating pyrolytic graphite target. The typical experimental setup of the pulsed laser deposited diamond-like carbon films with the presence of the magnetic field is schematically shown in Fig. 1.

In this study, a magnetic field with direction (central) perpendicular to substrate surface and parallel to the plume expansion axis was incorporated into the conventional PLD technique. Two cylindrical-shaped Nd–Fe–B permanent magnets with similar diameter of 45 mm and thickness of 10 and 20 mm were used in order to produce two different magnetic fields with surface magnetic flux densities of about B_1 = 220 and B_2 = 350 mT, respectively. The magnet with larger thickness produces a stronger magnetic field. The used magnets were directly adjoined on the substrate holder and the substrates were just placed on the surfaces of the magnets. All DLC films were deposited by 10,000 laser pulses at room temperature (RT) and the target to substrate distance was about 45 mm. The magnetic flux density distribution normal to magnet surface for two magnetic fields which was measured by Gaussmeter is shown in Fig. 2. It is observed that the magnetic flux density decreases with the distance from the magnet surface and the magnet surface (substrate position) exhibits a higher magnetic filed. Three series of DLC films were prepared with different deposition conditions. A series of thin films were deposited by conventional PLD technique in the absence of magnetic field (DLC sample). Two other films were deposited with the application of two magnetic fields with different strengths, one of which was under a weaker external magnetic field (B_1-DLC sample) and the other under a stronger magnetic field (B_2-DLC sample).

Raman spectroscopy (excitation wavelength of 532 nm and a power of up to 2 mW) and X-ray photoelectron spectroscopy (XPS: Specs model EA10 plus) were used to study the structural properties and chemical bonding of the samples. Thickness, surface morphology of the samples were investigated using field emission scanning electron microscopy (FE-SEM: Hitachi model S4460) and atomic force microscopy (AFM: Park Scientific Instruments, AUTOPROBE CP). The mechanical properties of the samples were measured by nanoindentation measurements (Compact Platform, Switzerland) using the continuous stiffness measurement (CSM) technique. The CSM technique is the most reliable method which has been widely used for evaluating the mechanical properties of thin films from the load–displacement curves of the indenter [11,29].

3. Results and discussion

3.1. Deposition rate (thickness) and film structure

The thickness of the samples was determined from the observation of the cross-section FE-SEM micrographs. Fig. 3 shows cross-section FE-SEM micrographs of the samples deposited in this work.

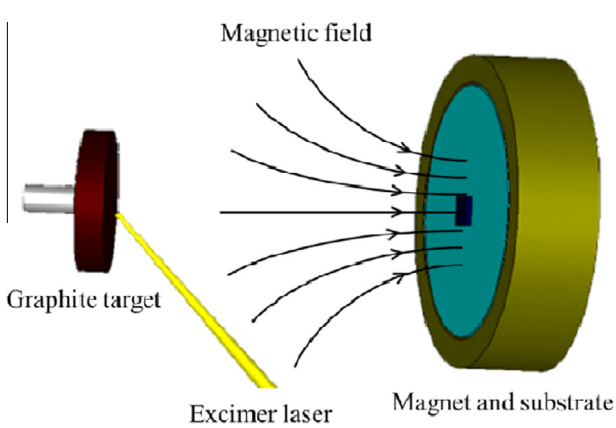

Fig. 1. The typical experimental setup of the pulsed laser deposition technique used for obtaining the diamond-like carbon films in the presence of magnetic field.

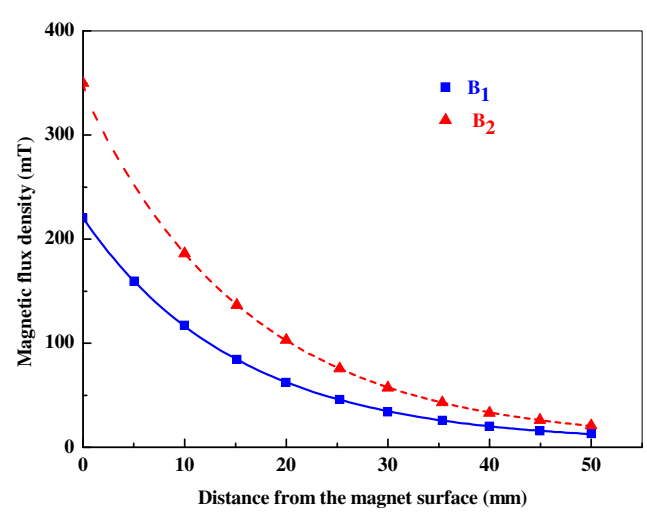

Fig. 2. The magnetic flux density distribution normal to magnets surfaces (measured by Gaussmeter) versus the distance from the magnetic surface for two magnetic fields.

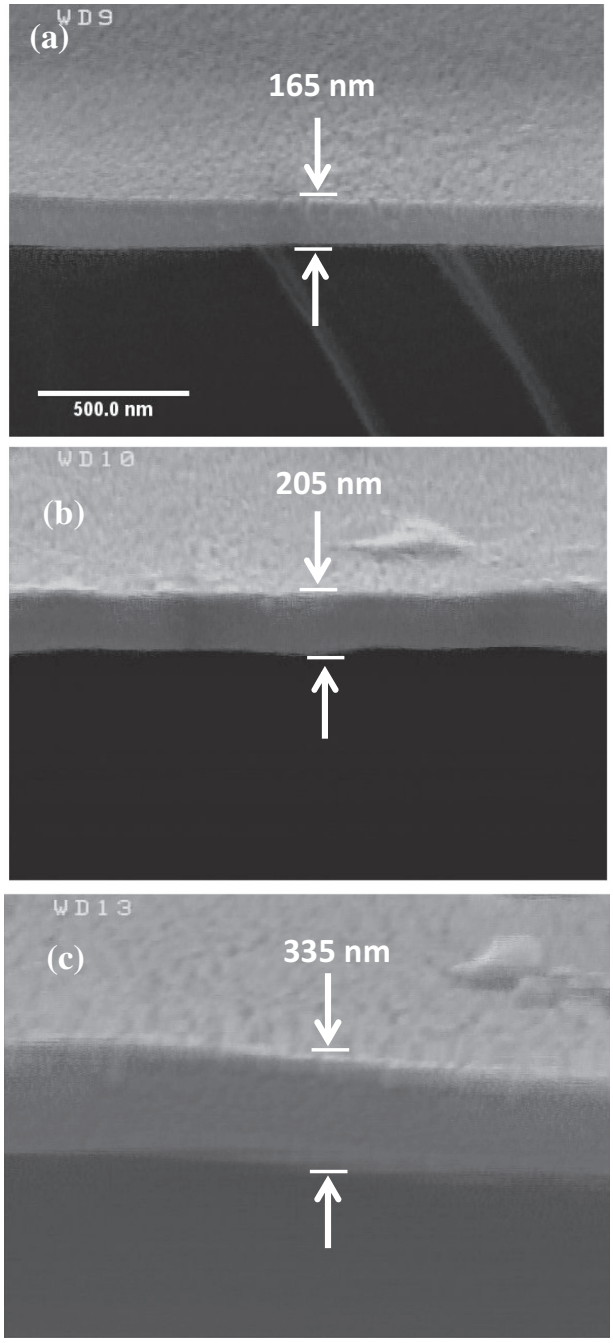

Fig. 3. Cross-section FE-SEM micrographs of (a) DLC, (b) B_1-DLC and (c) B_2-DLC samples.

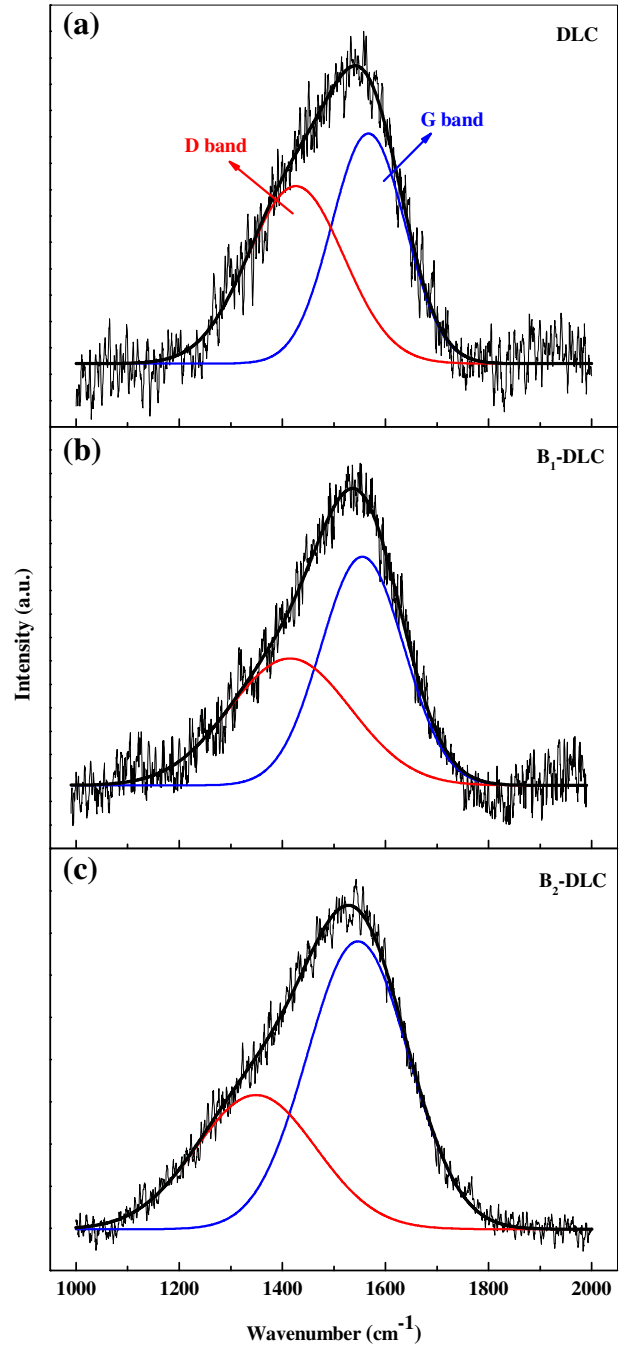

Fig. 4. Raman spectra for (a) DLC, (b) B_1-DLC and (c) B_2-DLC samples.

The results of thickness and deposition rate (thickness/pulse number) for samples deposited in this work are shown Table 1.

The thickness and deposition rate increase with the magnetic field. The thickness and deposition rate significantly increase when the stronger magnetic field (B_2) is applied. Raman spectroscopy is a standard non-destructive technique to obtain the microstructural information and the nature of bonding structure in the amorphous carbon thin films [30–33]. Usually, amorphous carbon thin films exhibit two main Raman bands in the wavenumber region of 1000–1800 cm^{-1} for visible excitation [31]. Fig. 4 shows the

Table 1
Thickness and deposition rate, variation of G-band position, I_D/I_G ratio and FWHM of G peak for deposited samples.

Sample	Thickness (nm)	Deposition rate (nm/pulse)	G-Peak position (cm^{-1})	I_D/I_G	FWHM of G peak
DLC	165	0.016	1567	1	167
B_1-DLC	205	0.020	1555	0.82	190
B_2-DLC	335	0.033	1546	0.55	231

Raman spectra for different samples. The Raman spectra in all samples consist of two characteristic (D and G) bands indicating the formation of DLC phase. The G peak is related to the stretching mode of all pairs of sp^2 carbon atoms in both rings and chains, whereas the D band is attributed to the breathing mode of sp^2 atoms in rings [31,34]. The Raman spectra were deconvoluted using Gaussian peaks and the parameters of interest were extracted. Table 1 shows the variation of G-band position, intensity ratio of D and G bands (I_D/I_G ratio) and full width at half maximum (FWHM) of G-band for DLC, B_1-DLC and B_2-DLC samples. It is seen that the G-peak position shifts to lower wavenumbers, I_D/I_G ratio decreases and FWHM of G-band increases with magnetic field increasing. The G band is centered at 1567 cm^{-1} for DLC sample which shifts to the lower wavenumbers of 1555 and 1546 cm^{-1} for B_1-DLC and B_2-DLC samples, respectively. This behavior is attributed to the enhanced sp^3 bonding in structure [3,35–39]. Moreover, the I_D/I_G ratio is 1 for DLC sample which decreases to 0.82 and 0.55 for B_1-DLC and B_2-DLC samples, respectively. The decrease in the I_D/I_G ratio indicates the decrease in the size and number of the sp^2 carbon clusters and increased sp^3 content [40–42]. FWHM of G-band is 167 for DLC sample which enhances to 190 and 231 for B_1-DLC and B_2-DLC samples, respectively. On the other hand, FWHM of G peak is related to the structural disorder (i.e., bond lengths and bond angles) and amorphization degree of the films. Therefore, the G-band becomes broader as the sp^2 clusters become more disordered [37,43]. In other words, the increase in FWHM of the G band with the magnetic field is attributed to enhanced amorphization degree and disordering the films [37,44,45]. Thus, the results obtained from shifting of G peak position, I_D/I_G ratio and FWHM value clearly reveal an enhancement in diamond-like character under applied magnetic field and the B_2-DLC sample exhibits the higher degree of diamond-like character (sp^3 bonding) and lowest value of sp^2 carbon clustering.

The XPS analysis was employed to estimate the surface bonding states in detail and obtain the sp^3 fraction in the deposited samples. Fig. 5 shows a typical survey scan spectrum for B_1-DLC sample. The observed peaks located at around 284.8 and 532.8 eV are due to the photoelectrons excited from the C1s and O1s core levels, respectively [46]. The presence of oxygen on the surface of the samples is related to some residual contaminations due to air exposure [46,47]. The feature in the binding energy range of 960–1030 eV is attributed to the carbon KVV Auger transitions [46].

Fig. 6 shows C1s high resolution XPS spectra for DLC, B_1-DLC and B_2-DLC samples. The XPS C1s spectra contain a large

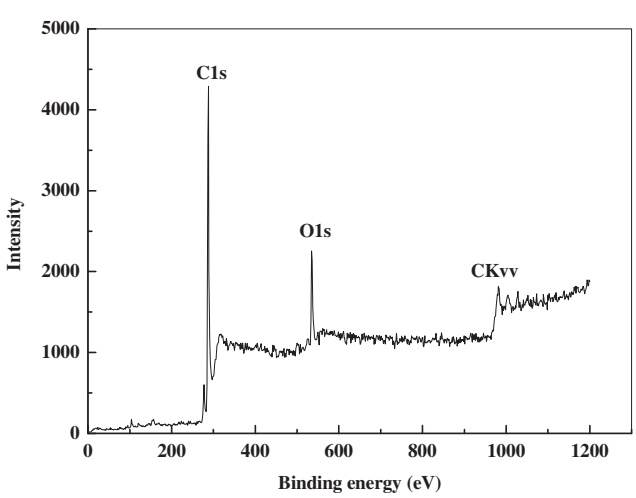

Fig. 5. A typical survey scan spectrum for B_1-DLC sample.

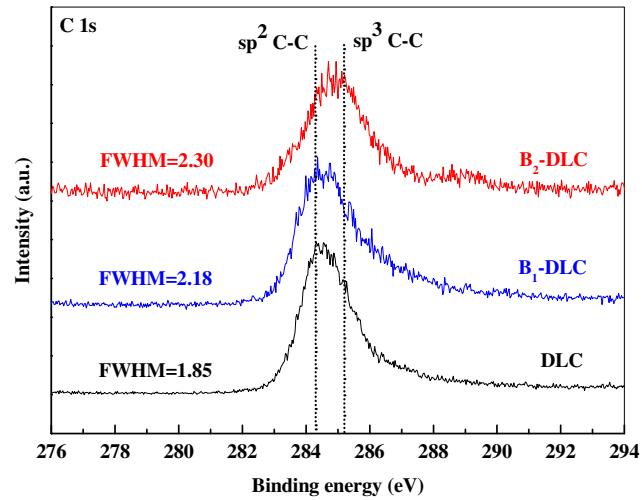

Fig. 6. C1s high resolution XPS spectra of DLC, B_1-DLC and B_2-DLC samples.

asymmetric peak suggesting the existence of carbon atoms in various bonding states [48]. The C1s peak position shifts toward higher binding energies, the peak width broadens and its shape becomes more symmetric with magnetic field, indicating the enhancement in the disordering and sp^3 bonding [49,50]. Moreover, FWHM of C1s spectra increases with an increase in the applied magnetic field. FWHM of DLC sample C1s spectrum is 1.85 which increases to 2.18 and 2.30 in B_1-DLC and B_2-DLC samples, respectively (Fig. 6). These results indicate an increase in the sp^3 content with an increase in magnetic field [51,52]. It has been reported in literature [50–52] that the sp^3 content vary with FWHM value. Higher FWHM value means higher sp^3 content. In principle, there are two significant reasons that are responsible for the broadening of C1s XPS spectra; namely the hybridization composition and the non-crystalline features [50]. The component representing tetrahedral bonding increases with the application of external magnetic field. Moreover, the structure of the film becomes more disordered. These lead to a broadening of C1s spectrum.

In order to estimate sp^3 fraction for the samples, the C1s XPS spectra were deconvoluted into three distinct Gaussian–Lorentzian peaks using Shirley backgrounds [53–55]. Fig. 7 shows the deconvoluted spectra for C1s peak of DLC, B_1-DLC and B_2-DLC samples. These peaks were centered at 284.3 ± 0.1 eV and 285.2 ± 0.1 eV, which were assigned to the C–C sp^2 hybridized carbon atoms and C–C sp^3 hybridized carbon atoms, respectively. The observed peak positions in this report are almost identical to those reported in the literature [11,53,56] for amorphous carbon films deposited by PLD. Another peak in the binding energy range of 286–289 eV is due to C–O (or C=O) bonds [46,47]. The sp^3 hybridized carbon atom fraction was then estimated as the ratio of the corresponding peak area to the total C1s peak area. The percentage of sp^3 hybridized carbon atom is about %30 for DLC sample which increases to about 44 and %65 for B_1-DLC and B_2-DLC samples, respectively (see Fig. 7). These results indicate that the sp^3 fraction increases with an increase in the magnetic field and the sample deposited under applied stronger magnetic field exhibits the highest value of sp^3 bonding. This result is in good agreement with the Raman spectroscopic analysis explained above. Other researchers have reported sp^3 content in the range of about 40–85% by FCVA process [50,57–60] through changing the ion energy, substrate temperature, and substrate bias voltage. Zhu et al. [50] have deposited the tetrahedral amorphous carbon (ta-C) films by FCVA process and reported its sp^3 content as a function of the

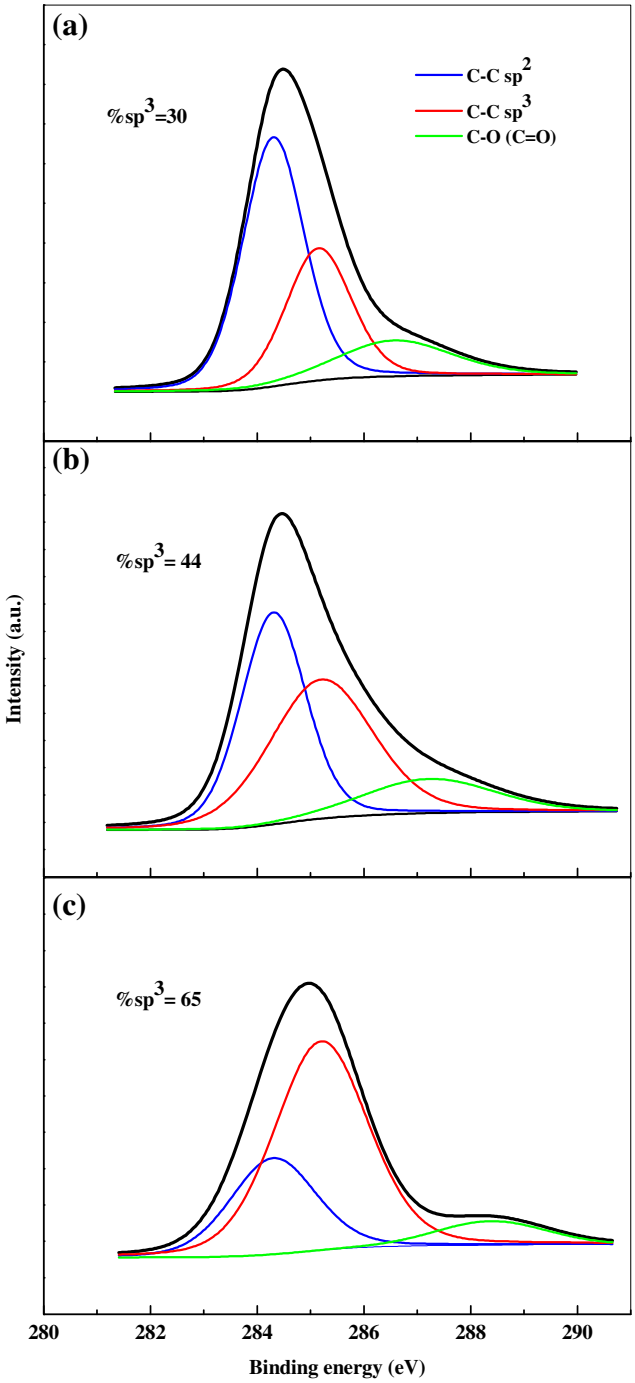

Fig. 7. Deconvoluted spectra of C1s peaks for (a) DLC, (b) B_1-DLC and (c) B_2-DLC samples.

substrate bias voltage. In that work the maximum sp^3 content of 70% (estimated by XPS analysis) at a bias voltage of −80 V was reported. Weiler et al. [57] have also obtained the maximum sp^3 content of about 75% at ion energy of 92 eV per carbon ion for the hydrogenated tetrahedral amorphous carbon (ta-C:H) film grown by FVCA. It seems that the B_2-DLC sample with 65% sp^3 content is comparable with the above reported results.

The observed increment in diamond-like character (sp^3 carbon bonding) and deposition rate (thickness) of the obtained samples may be explained by an enhanced ionization of the carbon species inside the plume and their confinement on the magnet (substrate position) due to the presence of magnetic field. Due to Lorentz force, the magnetic field affects the charged particles in the plume. It is known that the electrons move in spiral trajectories in the magnetic field and their collision probabilities with neutral carbon atoms are increased. This increases the possibility of the ionization of the carbon growth species in the plume leading to enhancement of the plasma density. Kobayashi et al. [25–27] found that an enhanced plume ionization from $SrTiO_3$, NiO and ZnO targets occurs with application of a magnetic field. They have assumed that a magnetic mirror effect occurs in the higher magnetic field zone (near the substrate), which contributes to the increment of interaction between electrons (confined by the magnetic field) and ablated species in the plume (see the distribution of the magnetic field shown in Fig. 2). It can be discussed that the plume ionization increases effectively, due to the collisions between the electrons reflected by the magnetic mirror effect from a high density magnetic field zone (substrates side) and neutral carbon atoms. This suggests that a large amount of ionized carbon species were produced. On other hand, due to convergence of the magnetic flux lines on the magnet (see Fig. 1), ionized carbon species move toward the substrate along the flux lines (confined) and leads to enhancement of the number of species depositing on the substrate surface. Thus, under application of magnetic field, an enhanced ionization of the carbon species inside the plume and confinement of the ionized species occurs which lead to production of highly ionized plasma consisting of carbon ions on the substrate position, which in turn promotes diamond-like character of the obtained samples. This fact was approved by Raman and XPS results.

The evolution of a dense sp^3-rich phase can be described by the sub-plantation model [14,58,61,62] which is based on the incident energetic ions penetrating the surface and providing subsurface growth. Under application of magnetic field, an increase in the amount of ionization of the carbon species enhances the ion bombardment of the growing film. This effect in turn increases the number of the carbon ions trapped in the subsurface interstitial sites. An increase in the amount of trapped energetic ion carbon species results in an increase of the local film density and induces internal compressive stresses, which is conducive to sp^3 hybridization via sub-plantation model [1,15,62,63]. It is observed that the thickness and deposition rate increases in the presence of the external magnetic field (Table 1). This improved deposition rate could be explained also by the enhancement of the density of carbon ionic species due to their confinement by the applied magnetic field. In other words, the confinement of increased ionized carbon species leads to the increase in the number of species arriving to the substrate position, which in turn increases the deposition rate [26]. One must note that the convergence of the magnetic flux lines and ionizing collision probability of energized electrons with neutral carbon atoms is proportional to the magnitude of the magnetic field. As a result, with the presence of the stronger magnetic field (B_2), ionized plasma density on the substrate surface enhances remarkably in comparison with the application of the weaker magnetic field (B_1). Therefore, the sample deposited under stronger external magnetic field (B_2-DLC) exhibits the higher sp^3 carbon bonding with an appreciable increment of deposition rate.

3.2. Morphological studies

The surface morphology of the samples obtained at the different deposition conditions were characterized by AFM technique. The AFM micrographs showed in Fig. 8 illustrate the significant changes in surface morphology and roughness of the obtained samples with and without application of the magnetic field. These micrographs clearly indicate the nanostructured morphology with the uniform and smooth surface for all the samples. In particular, the overall surface roughness values of all these samples

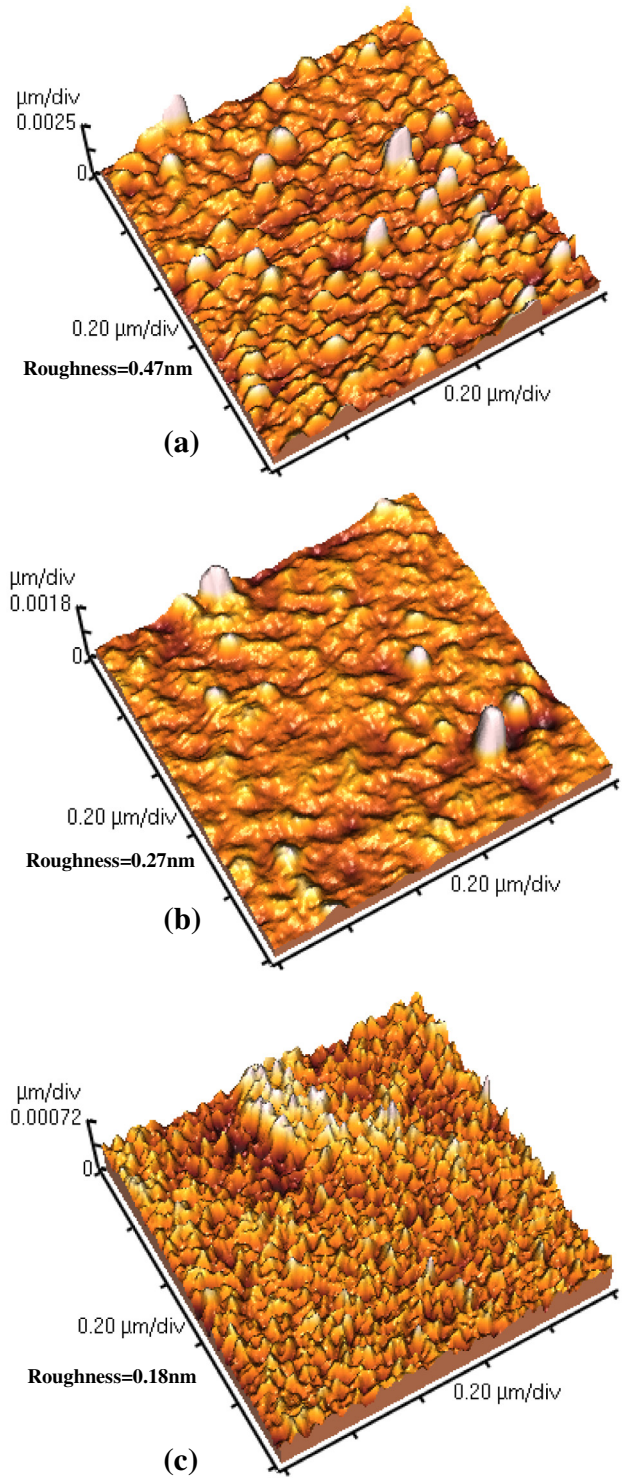

Fig. 8. AFM micrographs of (a) DLC, (b) B_1-DLC and (c) B_2-DLC samples.

(estimated by averaging on 1000 nm × 1000 nm area) were found to be less than 0.5 nm.

The morphology shown in Fig. 8 suggests that the surface of the DLC sample contains a large number of fine asperities and is relatively rougher than B_1-DLC and B_2-DLC samples. In contrast, with application of the external magnetic field during deposition, the features on the morphology change and the samples become smoother with a denser microstructure, which is confirmed by roughness analysis (see surface roughness value in Fig. 8). Moreover, the sample deposited under stronger magnetic field (B_2-DLC) has a much smoother surface and exhibits the lower surface roughness (Fig. 8c). The average surface roughness value of the DLC sample is 0.47 nm, which decrease to 0.27 and 0.18 nm for B_1-DLC and B_2-DLC samples, respectively. These roughnesses are in the range of those for the ta-C films deposited using FCVA [58]. Chhowalla et al. [58] reported roughness values in the range of 0.3–0.4 nm as a function of the deposition temperature for the ta-C films deposited using FCVA process. The improvement of the surface morphology and reduction of the surface roughness can be attributed to decrease of size and amount of sp^2 clusters and increase of the degree of diamond-like phase as confirmed by Raman and XPS results [16,44,62,64]. It has been reported by Lifshitz et al. [62,64] that there is a clear correlation between surface roughness and the degree of diamond-like (sp^3 bonding) character; i.e., the roughness decrease with an reduction in the amount of graphitic (sp^2) content.

3.3. Mechanical properties

The nanoindentation technique was used to characterize the mechanical properties of the samples obtained. Fig. 9 indicates load versus displacement curves at maximum indentation load of 1 mN for deposited samples. From these curves, it is observed that the DLC sample has broader hysteresis curve and lower recovery during unloading. On other hand, the B_1-DLC and B_2-DLC samples reveal lower hysteresis between loading–unloading curves and higher recovery during unloading. Furthermore, the hysteresis decreases and recovery enhances with increasing magnetic field. It is evident from Fig. 9 that the DLC sample exhibits maximum penetration depth and residual penetration depth. However, B_1-DLC and B_2-DLC samples have lower penetration depth and residual penetration depth and these characteristics decrease with increasing magnetic field. The observed decrease in hysteresis, penetration depth and residual penetration depth and the observed enhancement in recovery may be attributed to enhanced diamond-like character of the samples induced by the magnetic field application as confirmed by XPS and Raman results.

The load–displacement curves are also used to determine the mechanical properties such as hardness (H), elastic modulus (E), plastic index parameter (H/E), elastic recovery ($\%ER$) and ratio of residual displacement after load removal with displacement at maximum load (h_{res}/h_{max}) of the deposited samples. In order to avoid substrate effects in the nanoindentation measurements, the indenter penetration depth for our samples did not exceed about

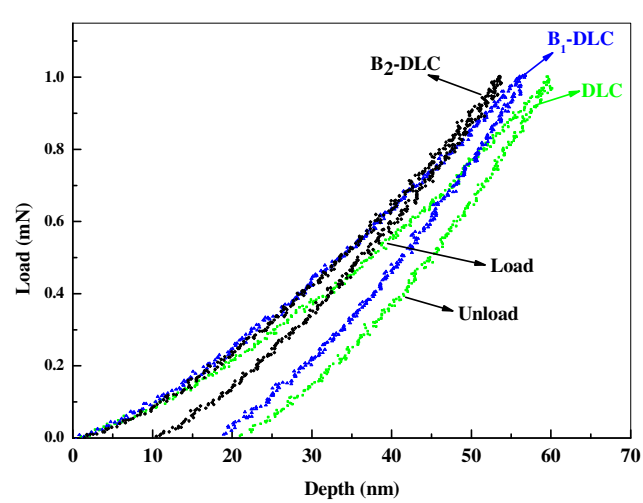

Fig. 9. Load versus displacement curves for obtained samples.

Table 2
Variations of H, E, H/E, $\%ER$ and h_{res}/h_{max} for deposited samples.

Sample	H (GPa)	E (GPa)	H/E	ER (%)	h_{res}/h_{max}
DLC	13.2	152	0.087	64	0.35
B_1-DLC	16.3	175	0.093	68	0.30
B_2-DLC	29.7	300	0.099	80	0.20

35% of the total film thickness [51,65–67]. The variations in the H, E, H/E, $\%ER$ and h_{res}/h_{max} values for various deposited samples are shown in Table 2. It is observed that the values of H and E in DLC sample is found to be lower than B_1-DLC and B_2-DLC samples and increase with increasing magnetic field. H is about 13.2 GPa for DLC sample which enhances to 16.3 and 29.7 GPa for B_1-DLC and B_2-DLC samples, respectively. Similar trend is observed for E value and is found to be 152 GPa for DLC sample which increases to the 175 and 300 GPa for B_1-DLC and B_2-DLC samples, respectively. Thus, it can be said that the application of the magnetic field in PLD technique enhances the H and E of deposited samples. The H value of B_2-DLC sample is similar to those reported by Motta et al. [59]. They have reported the H value in the range of 26–30 GPa as a function of the substrate bias voltage for the ta-C films deposited by FCVA process. Xu et al. [60] reported better H value in the range of 34–42 GPa as a function of the ion energy by FCVA process. The E value of B_2-DLC sample is also close to that reported by Weiler et al. [57] for ta-C:H film deposited by FVCA. They have reported the maximum E value of 288 GPa at the ion energy of 92 eV per carbon ion. Other report by Xu et al. [60] indicates the E values ranging from 295 to 345 GPa as a function of impinging carbon ion energy for ta-C films (60 nm thickness) deposited by FVCA process.

H and E are strongly depended on the microstructural and sp^3 bonding in the structure [11,68]. Observed increase in H and E with the application of magnetic field can be correlated to the magnetic field incorporation in PLD technique which enhances the formation strong sp^3 bonding and promotes the diamond-like structure (see Table 1 and Fig. 7). B_2-DLC film exhibits an improved diamond-like character, with a higher proportion of sp^3 fraction that lead to higher H and E values. Thus, the application of external magnetic field in PLD can be used to obtain high quality samples with improved mechanical properties.

Besides H and E, the wear resistance is another important property for amorphous carbon films. The plastic index parameter (H/E) explains elastic–plastic characteristics and is an indirect measure of wear resistance [69]. For DLC coatings, the H/E ratio variation is in the range of 0–0.1. The lower ratio (0) indicates the elastic–plastic behavior and the upper one (0.1) indicates the elastic behavior. On other hand, a very high value of H/E is required for high wear resistance DLC coatings [69]. The values of H/E for DLC, B_1-DLC and B_2-DLC samples is found to be about 0.087, 0.093 and 0.099, respectively (see Table 2). It is observed that the H/E ratio increases with the application and increasing the magnetic field during deposition. The minimum value of H/E ratio of DLC sample indicates that more fraction of the mechanical work is dissipated during plastic deformation and hence a large plastic strain is expected [51,70]. On the other hand, the higher value of H/E ratio in B_2-DLC samples is related to highly sp^3 bonding or an enhanced diamond-like structure, lesser plastic deformation and hence higher wear resistance [51]. Therefore, the sample deposited under stronger applied magnetic filed (B_2-DLC sample) seems to be more beneficial for fabrication a hard and high wear resistant coatings which can be used for the magnetic storage media.

Elastic recovery ($\%ER$) and h_{res}/h_{max} are other important mechanical parameter, which also provide information about the elastic and plastic behaviors and quality of the coatings [71]. $\%ER$ of the deposited samples can be calculated by the following relation:

$$\%ER = \frac{(h_{max} - h_{res})}{h_{max}} \times 100 \quad (1)$$

As can be seen in Table 2, $\%ER$ in DLC sample (about 64%) is found to be lower than B_1-DLC and B_2-DLC samples. It can be seen that the $\%ER$ in the sample deposited under applied magnetic field gets enhanced from about 68% to 80% with increasing magnetic field from B_1 to B_2 (Table 2). The results of $\%ER$ are in good agreement with the similar results for H. The h_{res}/h_{max} ratio variation is in the range of 0–1 for DLC coatings. The lower limit (0) and upper limit (1) is related to the elastic and plastic behavior, respectively. The value of h_{res}/h_{max} ratio in DLC, B_1-DLC and B_2-DLC samples is found to be 0.35, 0.30 and 0.20, respectively (see Table 2). The h_{res}/h_{max} results are also in good agreement with $\%ER$ results. The maximum value of $\%ER$ together with minimum value of h_{res}/h_{max} ratio in B_2-DLC sample seems to be in relation with the high sp^3 content (diamond-like bonding) as revealed by Raman and XPS results. Finally, it can be said that the mechanical properties of the obtained samples are strongly depended on the applied external magnetic field, sp^3 content and nature of plasma. All the mechanical parameters such as H, E, H/E, $\%ER$ and h_{res}/h_{max} improve for samples deposited under applied magnetic field. Particularly, we observed the appreciable improved mechanical properties in B_2-DLC sample (the sample deposited under stronger applied magnetic field). These attractive mechanical properties make our developed method desirable for fabrication of diamond-like carbon thin films which are a better candidate for mechanical and tribological applications. On other hand, magnetically-assisted PLD is quite general, very simple and can be employed as a powerful, cost effective ion-based method for the deposition of a wide range of metals, alloys and compounds by simple applying the magnetic field of a permanent magnet.

4. Conclusions

In this work, DLC thin films were deposited on Si-(100) substrates using a magnetically-assisted PLD technique and their microstructure, morphology, mechanical properties and deposition rate were studied. The following conclusions can be drawn from this work:

- It is found that the deposition rate increase under application of an external magnetic field.
- The results of Raman and XPS analysis indicated that the diamond like character and sp^3 bonding enhance under applied external magnetic field.
- AFM results indicate that the morphology features changes with magnetic field application and a denser microstructure, smoother surface with lower surface roughness value obtained under these conditions.
- Nanoindentation measurements indicate that the incorporation of an external magnetic field with conventional PLD technique improves the mechanical properties of the obtained DLC thin films.

However, it seems that more systematic works under application of wide range of magnetic fields with different strengths are required for in-depth understanding the effect of magnetic field and mechanism of evolution of DLC thin film in presence of external magnetic fields.

References

[1] J. Robertson, Diamond-like amorphous carbon, Mater. Sci. Eng., R 37 (4) (2002) 129–281.
[2] H.-S. Zhang, J.L. Endrino, A. Anders, Comparative surface and nano-tribological characteristics of nanocomposite diamond-like carbon thin films doped by silver, Appl. Surf. Sci. 255 (5) (2008) 2551–2556.
[3] T. Santra, C. Liu, T. Bhattacharyya, P. Patel, T. Barik, Characterization of diamond-like nanocomposite thin films grown by plasma enhanced chemical vapor deposition, J. Appl. Phys. 107 (12) (2010) 124320.
[4] W. Zhang, A. Tanaka, B. Xu, Y. Koga, Study on the diamond-like carbon multilayer films for tribological application, Diam. Relat. Mater. 14 (8) (2005) 1361–1367.
[5] A. Mousinho, R. Mansano, M. Massi, J. Jaramillo, Micro-machine fabrication using diamond-like carbon films, Diam. Relat. Mater. 12 (3) (2003) 1041–1044.
[6] A.-S. Loir, F. Garrelie, C. Donnet, J.-L. Subtil, M. Belin, B. Forest, et al., Mechanical and tribological characterization of tetrahedral diamond-like carbon deposited by femtosecond pulsed laser deposition on pre-treated orthopaedic biomaterials, Appl. Surf. Sci. 247 (1) (2005) 225–231.
[7] M. Morshed, B. McNamara, D. Cameron, M. Hashmi, Effect of surface treatment on the adhesion of DLC film on 316L stainless steel, Surf. Coat. Technol. 163 (2003) 541–545.
[8] F. Piazza, D. Grambole, D. Schneider, C. Casiraghi, A. Ferrari, J. Robertson, Protective diamond-like carbon coatings for future optical storage disks, Diam. Relat. Mater. 14 (3) (2005) 994–999.
[9] N. Xu, S.H. Tsang, E.H.T. Teo, X. Wang, C.M. Ng, B. kang Tay, Effect of initial sp^3 content on bonding structure evolution of amorphous carbon upon pulsed laser annealing, Diam. Relat. Mater. 30 (2012) 48–52.
[10] A. Grill, Diamond-like carbon: state of the art, Diam. Relat. Mater. 8 (2) (1999) 428–434.
[11] M. Tabbal, P. Merel, M. Chaker, M. El Khakani, E. Herbert, B. Lucas, et al., Effect of laser intensity on the microstructural and mechanical properties of pulsed laser deposited diamond-like-carbon thin films, J. Appl. Phys. 85 (7) (1999) 3860–3865.
[12] A. Jayatissa, F. Sato, N. Saito, Y. Hirano, K. Takizawa, Characterization of diamond-like carbon clusters deposited by pulsed ArF laser deposition, Carbon 38 (8) (2000) 1145–1151.
[13] Y. Lifshitz, Hydrogen-free amorphous carbon films: correlation between growth conditions and properties, Diam. Relat. Mater. 5 (3) (1996) 388–400.
[14] Y. Lifshitz, S. Kasi, J. Rabalais, W. Eckstein, Subplantation model for film growth from hyperthermal species, Phys. Rev. B 41 (15) (1990) 10468.
[15] D. McKenzie, D. Muller, B. Pailthorpe, Compressive-stress-induced formation of thin-film tetrahedral amorphous carbon, Phys. Rev. Lett. 67 (6) (1991) 773.
[16] Z. Tang, Z. Zhang, K. Narumi, Y. Xu, H. Naramoto, S. Nagai, et al., Effect of mass-selected ion species on structure and properties of diamond-like carbon films, J. Appl. Phys. 89 (3) (2001) 1959–1964.
[17] Y. Miyagawa, H. Nakadate, M. Ikeyama, S. Nakao, S. Miyagawa, Dynamic MC simulation for aC: H deposition in methane plasma based on subplantation model, Diam. Relat. Mater. 12 (3) (2003) 927–930.
[18] H.-S. Zhang, K. Komvopoulos, Direct-current cathodic vacuum arc system with magnetic-field mechanism for plasma stabilization, Rev. Sci. Instrum. 79 (7) (2008) 073905.
[19] N. Wang, K. Komvopoulos, Incidence angle effect of energetic carbon ions on deposition rate, topography, and structure of ultrathin amorphous carbon films deposited by filtered cathodic vacuum arc, Magn. IEEE Trans. 48 (7) (2012) 2220–2227.
[20] B. Tay, Z. Zhao, D. Chua, Review of metal oxide films deposited by filtered cathodic vacuum arc technique, Mater. Sci. Eng., R 52 (1) (2006) 1–48.
[21] A. Anders, W. Fong, A.V. Kulkarni, F.W. Ryan, C.S. Bhatia, Ultrathin diamond-like carbon films deposited by filtered carbon vacuum arcs, Plasma Sci. IEEE Trans. 29 (5) (2001) 768–775.
[22] A. Anders, Energetic deposition using filtered cathodic arc plasmas, Vacuum 67 (3) (2002) 673–686.
[23] A. Sikora, F. Garrelie, C. Donnet, A. Loir, J. Fontaine, J.C. Sanchez-Lopez, et al., Structure of diamondlike carbon films deposited by femtosecond and nanosecond pulsed laser ablation, J. Appl. Phys. 108 (11) (2010) 113516.
[24] F. Garrelie, A. Loir, C. Donnet, F. Rogemond, R. Le Harzic, M. Belin, et al., Femtosecond pulsed laser deposition of diamond-like carbon thin films for tribological applications, Surf. Coat. Technol. 163 (2003) 306–312.
[25] M. Tachiki, T. Kobayashi, Manipulation of laser ablation plume by magnetic field application, Jpn. J. Appl. Phys. 38 (6R) (1999) 3642.
[26] T. Kobayashi, H. Akiyoshi, M. Tachiki, Development of prominent PLD (Aurora method) suitable for high-quality and low-temperature film growth, Appl. Surf. Sci. 197 (2002) 294–303.
[27] S. Yata, Y. Nakashima, T. Kobayashi, Improved crystallinity of ZnO thin films grown by the 'Aurora PLD method', Thin Solid Films 445 (2) (2003) 259–262.
[28] M. Tachiki, T. Hosomi, T. Kobayashi, Room-temperature heteroepitaxial growth of NiO thin films using pulsed laser deposition, Jpn. J. Appl. Phys. 39 (4R) (2000) 1817.
[29] W.C. Oliver, G.M. Pharr, An improved technique for determining hardness and elastic modulus using load and displacement sensing indentation experiments, J. Mater. Res. 7 (06) (1992) 1564–1583.
[30] W. Cui, Q. Lai, L. Zhang, F. Wang, Quantitative measurements of sp^3 content in DLC films with Raman spectroscopy, Surf. Coat. Technol. 205 (7) (2010) 1995–1999.
[31] A. Ferrari, J. Robertson, Interpretation of Raman spectra of disordered and amorphous carbon, Phys. Rev. B 61 (20) (2000) 14095.
[32] A. Ferrari, J. Robertson, Resonant Raman spectroscopy of disordered, amorphous, and diamondlike carbon, Phys. Rev. B 64 (7) (2001) 075414.
[33] F. Rose, N. Wang, R. Smith, Q.-F. Xiao, H. Inaba, T. Matsumura, et al., Complete characterization by Raman spectroscopy of the structural properties of thin hydrogenated diamond-like carbon films exposed to rapid thermal annealing, J. Appl. Phys. 116 (12) (2014) 123516.
[34] P.K. Chu, L. Li, Characterization of amorphous and nanocrystalline carbon films, Mater. Chem. Phys. 96 (2) (2006) 253–277.
[35] A. Champi, F. Marques, Structural changes in amorphous carbon nitride films due to bias voltage, Thin Solid Films 501 (1) (2006) 362–365.
[36] H. Jiang, X. Tian, S. Yang, R. Fu, P. Chu, Structure and mechanical properties of diamondlike carbon films produced by hollow-cathode plasma deposition, J. Vac. Sci. Technol., A 26 (5) (2008) 1149–1153.
[37] M. Tamor, W. Vassell, Raman "fingerprinting" of amorphous carbon films, J. Appl. Phys. 76 (6) (1994) 3823–3830.
[38] D. Beeman, J. Silverman, R. Lynds, M. Anderson, Modeling studies of amorphous carbon, Phys. Rev. B 30 (2) (1984) 870.
[39] S. Gayathri, N. Kumar, R. Krishnan, S. AmirthaPandian, T. Ravindran, S. Dash, et al., Impact of laser power density on tribological properties of Pulsed Laser Deposited DLC films, AIP Adv. 3 (12) (2013) 2113.
[40] P. Yang, J. Chen, Y. Leng, H. Sun, N. Huang, P. Chu, Effect of annealing on structure and biomedical properties of amorphous hydrogenated carbon films, Surf. Coat. Technol. 186 (1) (2004) 125–130.
[41] J. Guo, Z. Sun, B. Tay, X. Sun, Field emission from modified nanocomposite carbon films prepared by filtered cathodic vacuum arc at high negative pulsed bias, Appl. Surf. Sci. 214 (1) (2003) 351–358.
[42] W. Gou, G. Li, X. Chu, B. Zhong, Effect of negative self-bias voltage on microstructure and properties of DLC films deposited by RF glow discharge, Surf. Coat. Technol. 201 (9) (2007) 5043–5045.
[43] C. Casiraghi, A. Ferrari, J. Robertson, Raman spectroscopy of hydrogenated amorphous carbons, Phys. Rev. B 72 (8) (2005) 085401.
[44] S. Kataria, S. Dhara, H.C. Barshilia, S. Dash, A. Tyagi, Evolution of coefficient of friction with deposition temperature in diamond like carbon thin films, J. Appl. Phys. 112 (2) (2012) 023525.
[45] S. Gayathri, N. Kumar, R. Krishnan, S. AmirthaPandian, T. Ravindran, S. Dash, et al., Impact of laser power density on tribological properties of Pulsed Laser Deposited DLC films, AIP Adv. 3 (12) (2013) 122113.
[46] T. Leung, W. Man, P. Lim, W. Chan, F. Gaspari, S. Zukotynski, Determination of the sp^3/sp^2 ratio of aC: H by XPS and XAES, J. Non-Cryst. Solids 254 (1) (1999) 156–160.
[47] W. Zhang, A. Tanaka, K. Wazumi, Y. Koga, Mechanical and tribological properties of Ar incorporated diamond-like carbon films, Thin Solid Films 416 (1) (2002) 145–152.
[48] E. Ech-Chamikh, A. Essafti, Y. Ijdiyaou, M. Azizan, XPS study of amorphous carbon nitride (aC: N) thin films deposited by reactive RF sputtering, Sol. Energy Mater. Sol. Cells 90 (10) (2006) 1420–1423.
[49] T. Ono, Y. Suda, M. Akazawa, Y. Sakai, K. Suzuki, Effects of oxygen and substrate temperature on properties of amorphous carbon films fabricated by plasma-assisted pulsed laser deposition method, Jpn. J. Appl. Phys. 41 (7R) (2002) 4651.
[50] J. Zhu, J. Han, X. Han, H.I. Schlaberg, J. Wang, Sp^3-rich deposition conditions and growth mechanism of tetrahedral amorphous carbon films deposited using filtered arc, J. Appl. Phys. 104 (1) (2008) 013512.
[51] S. Kumar, N. Dwivedi, C. Rauthan, Investigation of radio frequency plasma for the growth of diamond like carbon films, Phys. Plasmas 19 (3) (2012) 033515 (1994-present).
[52] O. Panwar, Y. Aparna, S. Shivaprasad, M.A. Khan, B. Satyanarayana, R. Bhattacharyya, XPS and XAES studies of as grown and nitrogen incorporated tetrahedral amorphous carbon films deposited by pulsed unfiltered cathodic vacuum arc process, Appl. Surf. Sci. 221 (1) (2004) 392–401.
[53] E. Riedo, F. Comin, J. Chevrier, F. Schmithusen, S. Decossas, M. Sancrotti, Structural properties and surface morphology of laser-deposited amorphous carbon and carbon nitride films, Surf. Coat. Technol. 125 (1) (2000) 124–128.
[54] P. Merel, M. Tabbal, M. Chaker, S. Moisa, J. Margot, Direct evaluation of the sp^3 content in diamond-like-carbon films by XPS, Appl. Surf. Sci. 136 (1) (1998) 105–110.
[55] H. Nakazawa, T. Kawabata, M. Kudo, M. Mashita, Structural changes of diamond-like carbon films due to atomic hydrogen exposure during annealing, Appl. Surf. Sci. 253 (9) (2007) 4188–4196.
[56] J. Diaz, G. Paolicelli, S. Ferrer, F. Comin, Separation of the sp^3 and sp^2 components in the C1s photoemission spectra of amorphous carbon films, Phys. Rev. B 54 (11) (1996) 8064.
[57] M. Weiler, S. Sattel, T. Giessen, K. Jung, H. Ehrhardt, V. Veerasamy, et al., Preparation and properties of highly tetrahedral hydrogenated amorphous carbon, Phys. Rev. B 53 (3) (1996) 1594.
[58] M. Chhowalla, J. Robertson, C. Chen, S. Silva, C. Davis, G. Amaratunga, et al., Influence of ion energy and substrate temperature on the optical and electronic properties of tetrahedral amorphous carbon (ta-C) films, J. Appl. Phys. 81 (1) (1997) 139–145.
[59] E.F. Motta, G.A. Viana, D.S. Silva, A.D. Cortes, F.L. Freire Jr., F.C. Marques, Structural, surface, and thermomechanical properties of intrinsic and argon implanted tetrahedral amorphous carbon, J. Vac. Sci. Technol., A 31 (2) (2013) 021502.

[60] S. Xu, B. Tay, H. Tan, L. Zhong, Y. Tu, S. Silva, et al., Properties of carbon ion deposited tetrahedral amorphous carbon films as a function of ion energy, J. Appl. Phys. 79 (9) (1996) 7234–7240.
[61] J. Robertson, Deposition mechanisms for promoting sp^3 bonding in diamond-like carbon, Diam. Relat. Mater. 2 (5) (1993) 984–989.
[62] Y. Lifshitz, G. Lempert, E. Grossman, Substantiation of subplantation model for diamondlike film growth by atomic force microscopy, Phys. Rev. Lett. 72 (17) (1994) 2753.
[63] M. Shakerzadeh, G. Loh, N. Xu, W. Chow, C. Tan, C. Lu, et al., Re-ordering chaotic carbon: origins and application of textured carbon, Adv. Mater. 24 (30) (2012) 4112–4123.
[64] Y. Lifshitz, G. Lempert, E. Grossman, I. Avigal, C. Uzan-Saguy, R. Kalish, et al., Growth mechanisms of DLC films from C^+ ions: experimental studies, Diam. Relat. Mater. 4 (4) (1995) 318–323.
[65] D. Liu, G. Benstetter, E. Lodermeier, J. Vancea, Influence of the incident angle of energetic carbon ions on the properties of tetrahedral amorphous carbon (ta-C) films, J. Vac. Sci. Technol., A 21 (5) (2003) 1665–1670.
[66] K.-I. Shimura, K. Baba, Microscale wear properties of ultrathin diamond-like carbon films, Jpn. J. Appl. Phys. 39 (6B) (2000) L626.
[67] H. Liu, Q. Xu, C. Wang, X. Zhang, B. Tang, Investigating the microstructure and mechanical behaviors of DLC films on AISI52100 bearing steel surface fabricated by plasma immersion ion implantation and deposition, Surf. Coat. Technol. 228 (2013) S159–S163.
[68] M. Chhowalla, A. Ferrari, J. Robertson, G. Amaratunga, Evolution of sp^2 bonding with deposition temperature in tetrahedral amorphous carbon studied by Raman spectroscopy, Appl. Phys. Lett. 76 (11) (2000) 1419–1421.
[69] C. Charitidis, Nanomechanical and nanotribological properties of carbon-based thin films: a review, Int. J. Refract. Met. Hard Mater. 28 (1) (2010) 51–70.
[70] N. Dwivedi, S. Kumar, H.K. Malik, Nanoindentation measurements on modified diamond-like carbon thin films, Appl. Surf. Sci. 257 (23) (2011) 9953–9959.
[71] N. Dwivedi, S. Kumar, H.K. Malik, Superhard behaviour, low residual stress, and unique structure in diamond-like carbon films by simple bilayer approach, J. Appl. Phys. 112 (2) (2012) 023518.